

Technical Note **TopoWind**

1. THE EQUATIONS SOLVED BY METEODYN WT

1.1. The Navier-Stokes equations

TopoWind solves the equations of Fluid Mechanics, i.e. the averaged equations of mass and momentum conservations (*Navier-Stokes equations*). When the flow is steady and the fluid incompressible, those equations become:

$$\frac{\partial U}{\partial x} + \frac{\partial V}{\partial y} + \frac{\partial W}{\partial z} = 0 \quad (1)$$

$$U \frac{\partial U}{\partial x} + V \frac{\partial U}{\partial y} + W \frac{\partial U}{\partial z} = -\frac{1}{\rho} \frac{\partial P}{\partial x} + \frac{\partial \overline{u^2}}{\partial x} + \frac{\partial \overline{uv}}{\partial y} + \frac{\partial \overline{uw}}{\partial z} \quad (2.1)$$

$$U \frac{\partial V}{\partial x} + V \frac{\partial V}{\partial y} + W \frac{\partial V}{\partial z} = -\frac{1}{\rho} \frac{\partial P}{\partial y} + \frac{\partial \overline{uv}}{\partial x} + \frac{\partial \overline{v^2}}{\partial y} + \frac{\partial \overline{vw}}{\partial z} \quad (2.2)$$

$$U \frac{\partial W}{\partial x} + V \frac{\partial W}{\partial y} + W \frac{\partial W}{\partial z} = -\frac{1}{\rho} \frac{\partial P}{\partial z} + \frac{\partial \overline{uw}}{\partial x} + \frac{\partial \overline{vw}}{\partial y} + \frac{\partial \overline{w^2}}{\partial z} \quad (2.3)$$

U, V, W are the components of the mean wind vector in a cartesian frame (x, y, z) where x and y are the horizontal coordinates and z the vertical coordinate. P is the mean pressure value and ρ the air density. $u, v,$ and w are the turbulence fluctuations components.

1.2. Turbulence modelling

The turbulent fluxes $\overline{uv}, \overline{uw}, \overline{vw}, \overline{u^2}, \overline{v^2}, \overline{w^2}$ are parameterized by using a one-equation K closure scheme.

The method is based on the hypothesis of proportionality between these correlations and the mean gradients. Thus:

$$-\overline{uv} = -v_T \frac{\partial U}{\partial y} \quad , \quad -\overline{uw} = -v_T \frac{\partial U}{\partial z} \quad , \quad -\overline{vw} = 0 \quad (3)$$

This turbulence model implies that a new transport equation is solved. Thus, the turbulent kinetic energy is resolved.

Such a model allows the solution to take into account the wake effects (*and will thus be more suitable when flow over complex terrains is studied*).

The speed scale is given by the square root of the turbulent kinetic energy k .

We got:

$$v_T = k^{1/2} L_T \quad (4)$$

The turbulent kinetic energy is a system variable, determined by an equation of transportation including production and dissipation of turbulence. This equation can be written:

$$U_j \frac{\partial k}{\partial x_j} = P_k - \varepsilon + \frac{\partial}{\partial x_j} \left[\left(\frac{v_T}{\sigma_k} \right) \frac{\partial k}{\partial x_j} \right] \quad (5)$$

Production P_k and dissipation ε are calculated by:

$$P_k = v_T \left(\frac{\partial U_i}{\partial x_j} + \frac{\partial U_j}{\partial x_i} \right) \frac{\partial U_j}{\partial x_j}$$

$$\varepsilon = C_\mu \frac{v_T}{L_T^2} k$$

The turbulent length scale is computed at the beginning of the calculation according to a model based on Yamada and Arritt [20]. This model takes into account the cases of stable or unstable thermal stratification:

$$L_T = \sqrt{2} S_m^{3/2} l \left\{ \begin{array}{l} \frac{1}{l} = \left(\frac{1}{l_0} + \frac{1}{\kappa z} \right), \text{ where } z = \text{height} \\ C_\mu = \frac{4S_m}{B_1} \\ S_m = \begin{cases} 1,96 \frac{(0,1912 - R_{if})(0,2341 - R_{if})}{(1 - R_{if})(0,2231 - R_{if})}, \text{ si } R_{if} < 0,16 \\ 0,085, \text{ si } R_{if} \geq 0,16 \end{cases} \\ B_1 = 16,6 \\ l_0 = 100m \\ \kappa = 0.41 \end{array} \right.$$

(R_{if} depending on thermal stratification)

1.3. Boundary conditions

Inlet conditions

The vertical profile of the mean wind speed at the computation domain inlet is given by the logarithmic law in the surface layer, and by the Ekman function above [16].

Turbulent kinetic energy is entering the domain with a constant value in the surface layer, and with an altitude-dependent value decreasing up to the upper boundary condition.

Ground conditions

The ground boundary condition used in **TopoWind** generates a sink in the momentum equations at the lower cells. Using the Monin-Obukhov theory, this term can be computed by the logarithmic law as a function of the mean wind speed at the first level cell, and of the real local roughness of the terrain.

This model includes the automatically modelling of the forest canopy. It is modelled by introducing of a sink term in the cells lying inside the forest (forest's height is supposed to be equal to 30 times the local roughness length).

This term acts as a drag force and enable to model the wake behind the forest and the wind profile above the forest [21]:

$$\rho \frac{DU}{Dt} = -\nabla p + \nabla \tau - \rho \cdot C_d \cdot U|U|$$

Where C_d is a coefficient which has been tuned on a French forest. According to the leaves density of the modelled forest, it may be interesting to vary this coefficient. This can be down in **TopoWind** by changing the forest density: three different forest densities can be chosen (*low, medium, high*). The low density will decrease the C_d coefficient which is used to in the drag force computation (*and the high density will increase it*).

Moreover, two forest models are included and, for each model, we use the following expressions for the calculation of the mixing length:

Robust model

The computation of the turbulent mixing length inside the forest volume is modified as follow

$$\frac{1}{l} = \begin{cases} \frac{1}{l_0} + \frac{1}{\kappa \cdot z}, & \text{if } z > d \\ \frac{1}{l_0} + \frac{1}{\kappa \cdot d}, & \text{if } z < d \end{cases}$$

Where:

- z is the height of the cell centre
- d is the canopy's height evaluated from the local roughness length

Dissipative model

The computation of the turbulent mixing length inside the forest volume is modified:

$$\frac{1}{l} = \begin{cases} \frac{1}{2}, & \text{if } z < d \\ (1-\alpha)\frac{1}{2} + \alpha\left(\frac{1}{l_0} + \frac{1}{\kappa \cdot z}\right), & \text{if } d < z < d + 15, \text{ with } \alpha = \frac{z-d}{15} \\ \frac{1}{l_0} + \frac{1}{\kappa \cdot z}, & \text{if } z > d + 15 \end{cases}$$

Where:

- z is the height of the cell centre
- d is the canopy's height evaluated from the local roughness length

For this "Dissipative model", an 15 meters extra high dissipation zone is used above the forest.

Moreover, a horizontal smoothing of the turbulent length is performed in order to avoid getting high gradients between cells in horizontal directions.

Finally, the dissipation term in the turbulent kinetic energy is modified as follow:

$$\varepsilon = \max(\varepsilon_{cc}, \varepsilon_{fd}), \text{ where } \begin{cases} \varepsilon_{cc} = C_{\mu} \frac{V_T}{L_T^2} k \\ \varepsilon_{fd} = C_d |U| k \end{cases}$$

1.3.2. Upper, lateral and outlet boundary conditions

A symmetry condition is applied at the lateral boundaries of the computational domain.

At the upper boundary, and at the outlet, an homogeneous pressure condition is applied.

1.4. Turbulence intensity computation

The turbulence intensity is defined as the ratio between the standard deviation and the mean of the wind speed.

In **TopoWind**, it is estimated by the ratio between the square root of the turbulent kinetic energy and the local speed of the flow.

2. MESH GENERATION

Step 1 : Surface grid generation

A cartesian grid with refinement at « **result points** » is generated. The expansion of grid cells dimensions is controlled, as well as, the aspect ratios in order to avoid convergence instabilities.

Step 2 : Volume grid generation

- Method of front propagation starting from the surface grid.
- Control of the line orthogonalities regarding the ground surface.
- Elliptic control of the distance between “vertical” lines.
- Optimisation of the couple (*orthogonality/verticality*)

3. MIGAL SOLVER

The MIGAL solver, developed by MFRDC has been regularly used for some years, and has been fully validated on number of academic cases ([1,2]).

MIGAL is an iterative linear equations solver which updates simultaneously the wind speed components as well as the pressure on the whole computational domain (“coupled resolution”). This method demands more storage capacity, but presents the advantage to dramatically increase the convergence process.

The discretized equations linear system, is transformed via an incomplete LU decomposition ILU(0) (see [2]). To improve the robustness of the solving, a preconditioner of type GMRES is used.

Moreover, MIGAL uses a multi-grid procedure which consists in solving successively the equations on different grid levels (from the finer one to the coarser one). This method accelerates the convergence of the low frequency errors, which are known to be the limiting factor in the convergence process. For the type of problem solved here, the tests have shown a better convergence for “V cycles” method than “W cycles method”.

A very precise description of numerical methods developed in MIGAL can be found at reference [2].

Compared to segregated, single grid methods, the benefit in convergence speed is a gain by a factor 5 or 10.

4. INTERPOLATION METHODS

4.1. Altitude data interpolation

The interpolation at the surface grid points is realized by an original method, called « by ray launch », allowing to avoid inconsistencies and smoothing observed, for instance in Spline methods.

4.2. Roughness data interpolation

The research of the roughness points is realized in the same manner as altitude points. However, the value affected to grid points is the value at the nearest roughness point.

4.3. Results interpolation

The techniques to interpolate at the result points, the values got at each computational grid point, has been developed by Meteodyn on the basis of coherence with the atmospheric boundary layer equations. This method presents the following advantages:

- Taking into account differences between horizontal and vertical scales in the atmospheric boundary layer.
- Rapidity thanks to the original algorithm.
- Taking into account roughness terrain characteristics for the interpolation in the vertical direction.

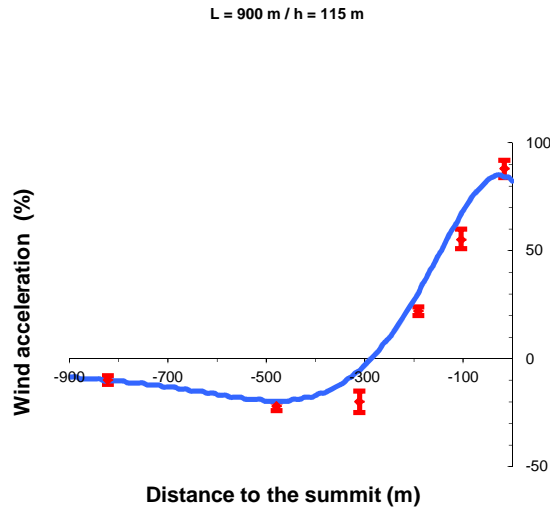
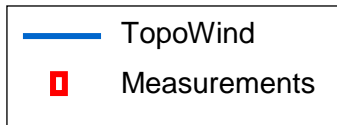
5. VALIDATIONS

6.1. Boundary conditions implementation / Friction laws at ground

This verification has been made with academic test cases: development of the boundary layer along a flat plane with inhomogeneous roughnesses. Theoretical usual profiles are well reproduced for mean wind speed, as well as turbulence intensity.

6.2. Two dimensional hills

We compare with wind-tunnel tests on a 2D Gaussian hill, with height 115 m and full length of about 900 m [10]. The figure shows the very good coherence between measurements and Meteodyn results.

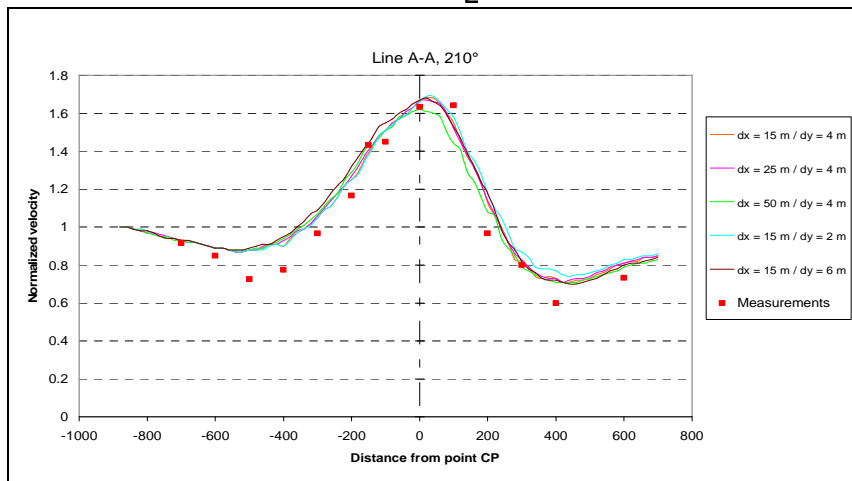


2D Gaussian hill: Comparison between measurements [10] and computations

6.3. Comparison with in situ measurements: The Askervein hill

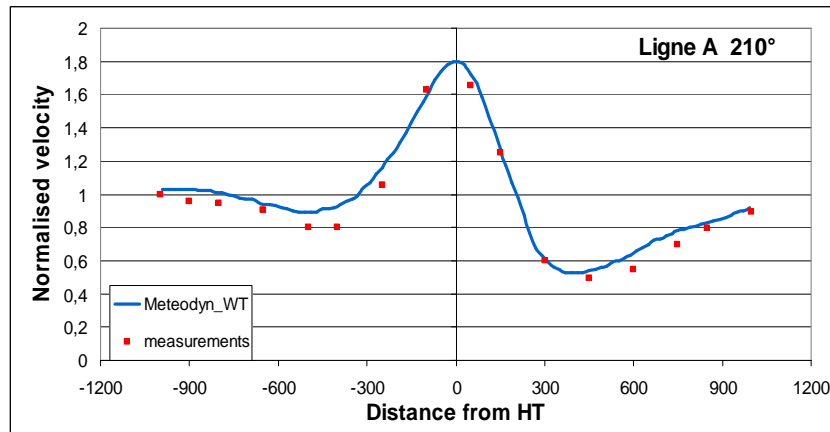
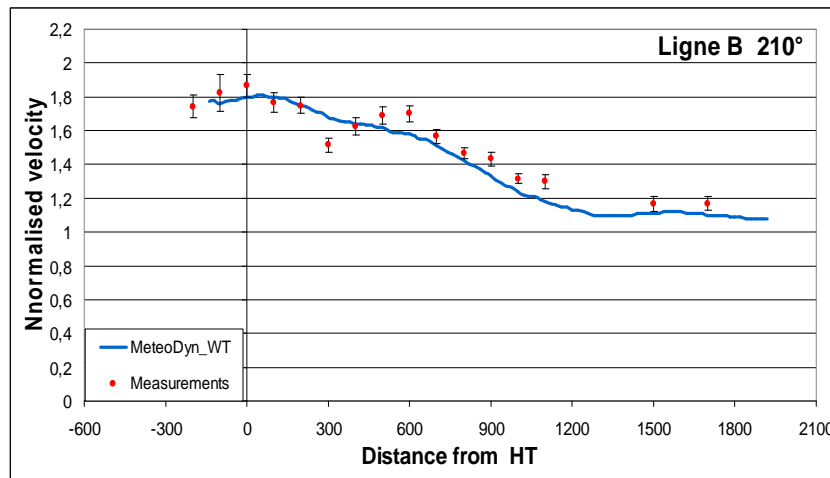
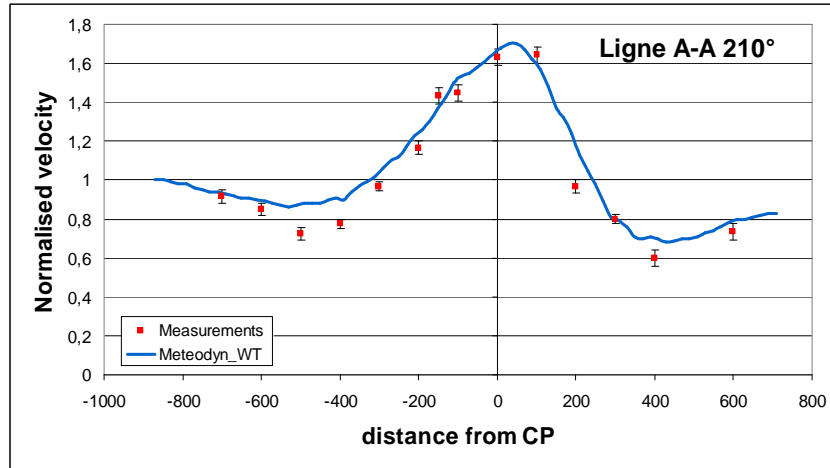
The atmospheric flow past the Askervein hill is a standard validation case. This site has been equipped with number of wind sensors, at 10 m height, along longitudinal and transversal lines [11,12]. The shape of the 126 meters high hill is ellipsoidal, with a great axis of 2 km, a little axis of 1 km.

Tests carried out in order to evaluate the mesh and domain dimension influences have shown that a domain of 10 km x 10 km, with a mesh resolution of 25 m in the horizontal directions and 4 m in the vertical one was the optimal conditions to solve the flow. For such a case, the number of volumic cells is 1 million. Convergence is reached in 30 minutes with a processor of 3 GHz.



Mesh sensitivity tests

The figures below show, for the 210 degrees direction, and the three measurement lines, the comparison between Meteodyn results and mean wind speed measurements.



Comparison between Meteodyn results and mean wind speed measurements

6.4. Comparison with in situ measurements: Koudia wind park (Morocco)

The flow past a mountainous site, the wind park of Koudia in Morocco, has been computed by La Compagnie du Vent (France) by using Meteodyn WT. Also, La Compagnie du Vent has analysed wind measurements on the site, during the years 1998 and 1999 [13].



Partial view of the Koudia wind park

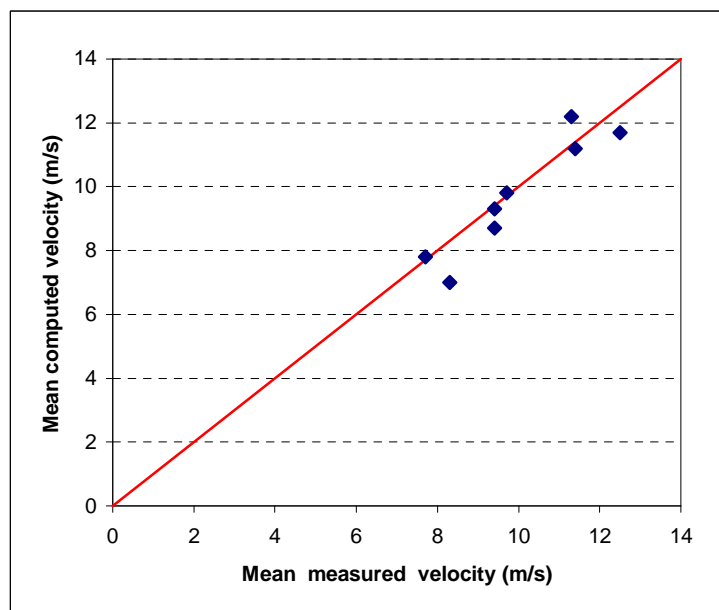
The analysis has consisted to calculate the ratio between the mean wind speed measured at 30 m height on 4 points, and the mean wind speed measured at a reference point at the same height (point K1). The distances from the test points to the reference point stand between 2 km and 7.5 km. Computations with the software WASP have been also conducted.

The following table allows to compare the mean wind speed (all directions included), computed by Meteodyn, by WASP, and measured. The error on the mean wind speed, which can reach 30 % with WASP, do not exceed 10 % with Meteodyn.

| | Meteodyn WT | WAsP |
|----------|--------------------|-------------|
| Point K4 | - 4 % | + 7 % |
| Point K5 | - 2 % | + 11 % |
| Point K6 | + 8 % | + 17 % |
| Point K7 | + 10 % | + 30 % |

Errors on computed mean wind speed at the Koudia wind park

The following figure sums up the whole results for the two main direction sectors (West and East).



Mean computed and measured velocities for all the four points and the two directional sectors

REFERENCES

- [1] Ferry M., 2000, "The MIGAL solver", Proc. Of the Phoenix Users Int. Conf., Luxembourg, 2000
- [2] Ferry M., 2002, "New features of the MIGAL solver", Proc. Of the Phoenix Users Int. Conf., Moscow, Sept. 2002
- [3] Duynkerke P.G., 1988, "Application of the E-e turbulence closure model to the neutral and stable atmospheric layer", vol. 45, 5, pp 865-880
- [4] H. Panofsky, J. A. Dutton, 1983 "Atmospheric turbulence, Models and Methods for Engineering Applications", University Park, Pennsylvania.
- [5] J.R. Garratt, 1992, *The Atmospheric Boundary Layer*, Cambridge University Press
- [6] CSTB, 1995, *Traité de Physique du Bâtiment, Tome 1 , Connaissances de base* , Editions CSTB, Paris
- [7] Eurocode 1, 2000, *Actions du vent et de la neige sur les structures*, AFNOR Paris.
- [8] P.A. Taylor, R.I. Sykes, P.J. Mason, 1989, On the parameterization of drag over small-scale topography in neutrally-stratified boundary-layer flow, *Boundary-Layer Meteorol.*, 48 (1989) 409-422
- [9] A.J Bowen, 1983, *The prediction of mean wind speeds above simple 2D hill shapes*, *Journal of Wind Engineering and Industrial Aerodynamics*.
- [10] O. Zeman, N. O. Jensen, 1987, *Modification of turbulence characteristics in flow over hills*, *Q.J.R. Meteorology Society*, vol 113., pp 55-80
- [11] Taylor et Teunissen, 1986, *The Askervein Hill project : overview and background data*, Atmospheric Environment Service, Downsview, Ontario, Canada
- [12] J.R.Slamon, A.J. Bowen, A.M. Hoff, R. Johnson, R.E. Mickle, P.A.Taylor, G. Tetzlaff and J.L. Walmsley , 1987, *The Askervein hill project :mean wind variations at fixed heights above ground*
- [13] La Compagnie du Vent, 2004, *Tests du code de calcul Meteodyn_WT sur le site de Koudia*, rapport interne
- [14] Businger J.A., Wingaard J.C., Izumi, Y., Bradley E.F., 1971, *Flux profile relationships in the atmospheric boundary layer*, *J. Atmos. Sci.*, vol.28, 181-189.
- [15] Monin A.S. and Yaglom A.M., 1973, *Statistical Fluid Mechanics*, Volume 1, MIT Press, Cambridge, UK.
- [16] J.R. Garratt (1992) *The atmospheric boundary layer*, Cambridge Atmospheric and space sciences series.
- [17] H.A. Panofsky, J.A. Dutton (1983) *Atmospheric turbulence, Models and Methods for Engineering Applications*, University Park, Pennsylvania.

[18] P.A. Taylor and H.W. Teunissen (1986) *The Askervein Hill project : overview and background data*, Atmospheric Environment Service, Downsview, Ontario, Canada

[19] Numerical Fluid Dynamics

[20] P. J. Hurley (1997) *An evaluation of several turbulence schemes for the prediction of mean and turbulent fields in complex terrain*

[21] A.N. Ross, S.B. Vosper *Neutral Turbulent flow over forested hills*